10.21611/qirt.2022.2005
QIRT'2022
16th Quantitative InfraRed Thermography Conference

Performance analysis of a microbolometer camera with and without Peltier temperature stabilizer

by M. Felczak*, T. Sosnowski**, M. Kastek**, R. Strąkowski*, J. Stępień***, B. Więcek*

* *Institute of Electronics, Lodz University of Technology, Poland*
** *Military University of Technology, Warsaw, Poland*
*** *Milton Essex, Warsaw, Poland*

Abstract

The article presents thermal modelling of a microbolometer detector inside the FPA (Focal Plane Array) camera. This modelling assumes heat transfer from/to the bolometer matrix through the multilayer structure. The Peltier cooler is one of the layer which enables the equalization and stabilization of the temperature below the FPA. The presented model allows to simulate the heat transfer by radiation between the matrix and an object and the impact of Peltier device on the FPA temperature. The parasitic radiation heat transfer between the detector and surrounding objects resulting in the non-uniformity of the generated signal is neglected. The model can estimate the performance deterioration of a microbolometer camera due to the non-ideal stabilization of the temperature by the Peltier cell.

1. Introduction

From the very beginning of the IR mirobolometer technology, scientists and manufacturers have searched for new ideas to improve detector performance [1], [2], [3], [4], [5]. One solution was a Peltier cooler or a temperature stabilizer integrated inside the detector package. Later, the Peltier device was replaced with a heater, which was eventually removed from the detector housing for reasons of cost and high power consumption.

Both users and manufacturers of microbolometer detectors believe that the Peltier cooler/stabilizer significantly helps to achieve higher sensitivity and the temperature uniformity of the array of IR detectors. Currently, there are bolometric sensors without cooling and heating devices with very good measurement parameters [1], [2], [4], [5].

This article attempts to verify the main arguments for and against the use of cooling or heating devices adjacent to the IR detector placed in the thermal path between the bolometer and the housing of the thermal imaging camera. All the work was done by modelling in the *Matlab* environment using the time-effective 1D simulation of heat transfer in the frequency domain [6], [7].

2. Simplified 1D thermal model of the microbolometer detector

The simplified 1D 5-layer structure of a microbolometer detector is shown in figure 1. The bolometer sensor itself consists of a 100 nm membrane coated with amorphous silicon *s-Si* or *VOx* and a layer of electrical connectors with a thickness of 2.5 μm. These electrical connectors were replaced in the model with a bulk-material layer with scaled-down thermal parameters.

For each $i-th$ layer of the thermal structure, heat is transfer from the source to the ambient according the Fourier-Kirchhoff equation (1).

$$\frac{\partial^2 T_i}{\partial x^2} - \frac{c_{vi}}{k_i}\frac{\partial T_i}{dt} = -\frac{q_{vi}}{k_i} \tag{1}$$

where: $c_{vi} = \rho_i \cdot c_i$ - thermal volumetric capacity, ρ_i - density, c_i - specific heat and k_i - thermal conductivity, q_{vi} - power density.

Equation (1) in Laplace domain for $s = j\omega$ takes form:

$$\begin{gathered}\frac{\partial^2 T_i}{\partial x^2} - \frac{T_i}{L^2} = -\frac{q_{vi}}{k_i} \\ L_i(j\omega) = \sqrt{\frac{k_i}{j\omega c_{vi}}}\end{gathered} \tag{2}$$

where L_i is characteristic length of the $i-th$ layer.

Analytical solution of (2) for the $i-th$ layer takes the form of equation (3).

$$T_i(j\omega) = A_i(j\omega)e^{-\frac{x}{L_i(j\omega)}} + B_i(j\omega)e^{\frac{x}{L_i(j\omega)}} + \frac{L_i^2(j\omega)}{k_i}q_{v,i} \tag{3}$$

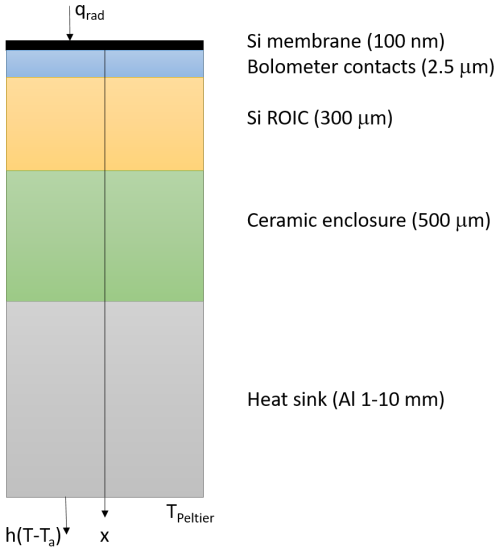

Fig. 1. *Simplified model of a 12 μm bolometer camera, out of scale*

The presented model describes the thermal system in the frequency domain [6], [7]. Thanks to this approach, it is possible to estimate the temperature of a thermal object as the response to any harmonic (sinusoidal) excitation.

In order to solve the thermal model (1), it is necessary to define boundary and interface conditions [7]. As shown in the figure 1, on the upper surface of the detector, heat is transferred to/from the environment only by radiation (q_{rad}). This is because the bolometer is encapsulated in a vacuum housing where convection cooling is practically reduced to zero.

On the bottom surface of the heat sink in of the considered model, cooling was assumed either by coupled convection and radiation (h_{case}) or by a strong heat flux caused by the constant temperature stabilized with the Peltier cell.

The upper bolometer surface boundary condition

$$-k_1 \frac{dT_1(0)}{dx} = q_{rad} \tag{4}$$

where q_{rad} denote the radiation heat flux emitted (or absorb) by an object.

The interface conditions between the layers for i=2-4

$$-k_i \frac{dT_i(d_i)}{dx} = -k_{i+1} \frac{dT_{i+1}(0)}{dx} \tag{5}$$

$$T_i(d_i) = T_{i+1}(0) \tag{6}$$

The boundary condition at the bottom of the heat sink

Convective or strong isothermal cooling is applied to the lower surface of the thermal mass attached to the detector, represented by the equations (7) and (8). The constant temperature cooling can be realized using a Peltier device equipped with a high-quality control system.

$$-k_n \frac{dT_5(d_5)}{dx} = hT_5(d_5) \tag{7}$$

or

$$T_5(d_5) = T_{Peltier} \tag{8}$$

The radiant heat flux q_{rad} emitted/absorb by an object and measured by a bolometric camera is given by the equation (9).

$$q_{rad} = \frac{\tau_{optics}}{4F^2 + 1} \int_{\lambda_1}^{\lambda_2} m(\lambda) d\lambda \tag{9}$$

where: spectral exitance $m(\lambda)$ integrated in absorption wavelength range of a camera, i.e. $\lambda_1 = 7\ \mu m$ and $\lambda_2 = 14\ \mu m$, τ_{optics} = 0.9 is transmission coefficient of a camera optical path and F is the aperture (F-number) of lens used.

In the case of heating or cooling the bolometer with the energy of the object's radiation, the thermal impedance determined in the frequency domain is an important and very helpful quantity for further analysis. It takes the form of equation (10) and can be represented graphically as the Nyquist plot [6], [7].

$$Z_{th}(j\omega) = \frac{T_{source}(j\omega)}{\sum_i P_i} \tag{10}$$

where: P_i denotes the power dissipated in the $i-th$ layer.

In the case of heating or cooling the bolometer by varying either the temperature of *Peltier* cold side $T_{Peltier}$ or the ambient T_a, it is worth to define the thermal gain k_{th} - equation (11).

$$k_{th}(j\omega) = \frac{T_{source}(j\omega)}{\Delta T} \tag{11}$$

where: ΔT is equal either $\Delta T_{Peltier}$ or ΔT_a.

3. Simulation results and discussion

The model of the bolometric detector has been implemented in the *MATLAB* environment. The values of the parameters selected for the simulation are shown in the table 1.

Since the heating of the detector is simulated with a 1D model, the problem arises of assessing the thermal parameters of the optical cavity layer under the microbolometer membrane which contains the electrical connectors of each detector in the system. It was assumed that the replaced both thermal conductivity and capacity is scaled down by the ratio of the cross-section of the surface of 2 electrical connectors and $(2 * S_{pin})$ the entire microbolometer (S_b). In this research it was assumed that $S_{pin} = 10^{-12}\ m^2$ and $S_b = 12x12 * 10^{12}\ m^2$.

Table 1. *Paramters values selected for simulation*

Parameter	Value
Bolometer detector size	640x480x12 μm
Bolometer detector thickness	100 nm
Bolometer optical cavity thickness	2.5 μm
ROIC thickness	300 μm
Ceramic enclose thickness	500 μm
Heat sink thickness	1 cm
Bolometer detector thermal conductivity	2 $W/m \cdot K$
Bolometer optical cavity thermal conductivity	0.28 $W/m \cdot K$
ROIC thermal conductivity	150 $W/m \cdot K$
Ceramic enclose thermal conductivity	20 $W/m \cdot K$
Heat sink thermal conductivity	210 $W/m \cdot K$
Bolometer detector thermal capacity	1.84*10^6 J/m^3K
Bolometer optical cavity thermal capacity	0.026*10^6 J/m^3K
ROIC thermal capacity	1.61*10^6 J/m^3K
Ceramic enclose thermal capacity	3.25*10^6 J/m^3K
Heat sink thermal capacity	2.43*10^6 J/m^3K
Heat transfer coefficient h	50 W/m^2K

The results of the model are presented in the form of the Nyquist plots of the thermal impedance and gain in figures 2 - 4. Figure 2 shows the thermal impedance calculated for excitation of the detector by the radiation power emitted or absorbed by the object.

Figure 3 shows the thermal gain k_{th} for the power delivered to the bottom of the heat sink (figure 2) by setting the cold side temperature of the Peltier cell.

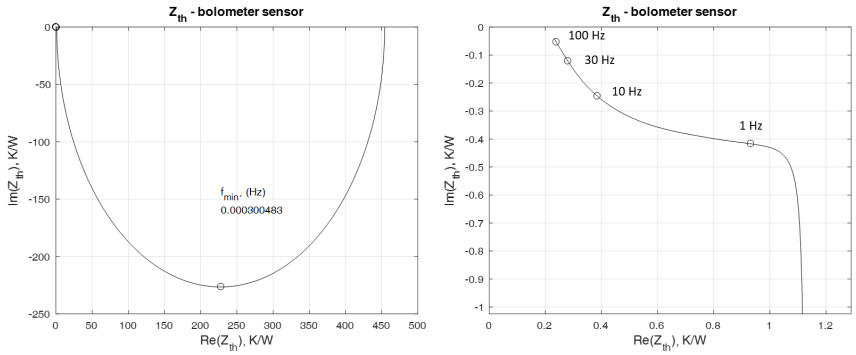

Fig. 2. *Thermal impedance of the bolometer matrix for the radiation power absorbed by the microbolometer*

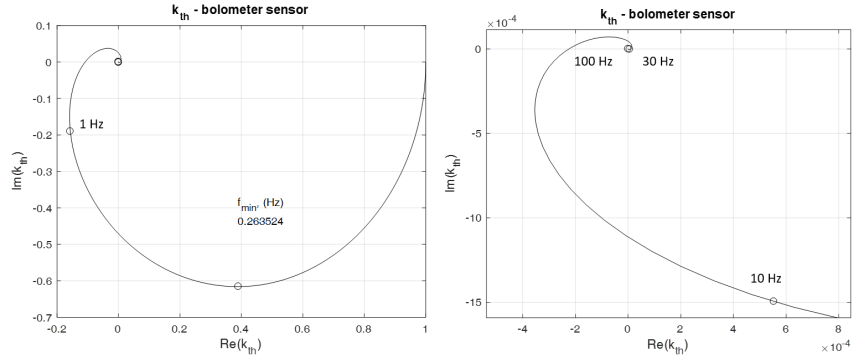

Fig. 3. *Thermal gain for the bolometer 640x480 matrix and the Peltier cell attached to the heat sink*

The thermal gain of the bolometer detector heated or cooled by the convection heat transfer is shown in figure 4

Thermal analysis of the bolometer matrix can lead to several conclusions. Temperature stabilization by the Peltier cell attached to the heat sink results in much less thermal inertia. This means that during start-up, the camera can be up and running in much less time. It significantly reduces the thermal drift caused by the ambient and heat sources inside the camera. On the other hand, the Peltier heat source has a greater effect on the bolometer itself. Consequently, the influence of the Peltier cell on the detector temperature value is much greater compared to the convective heat transfer between the detector and the environment.

The quantitative modelling results are presented in the table 2. In order to obtain comparable results, it was assumed that for all 3 modelled heat transfer cases, the detector temperature change was caused by the temperature change of the respective heat source by 1^oC.

Table 2. *Values of the temperature of the bolometer for different heat sources and different frequency of the excitation - simulation*

Bolometer heat source	f_{min} mK	1 Hz mK	10 Hz mK	30 Hz mK	100 Hz mK
Radiation	8.2	$2.6 * 10^{-2}$	$1.2 * 10^{-2}$	$7.8 * 10^{-3}$	$6.3 * 10^{-3}$
Peltier	729.0	246.7	1.6	$6.3 * 10^{-3}$	$1.4 * 10^{-7}$
Free convection	707.8	$2.1 * 10^{-1}$	$4.5 * 10^{-4}$	$1.0 * 10^{-6}$	$1.3 * 10^{-11}$

As a typical bolometer camera operates at a frame rate of 30 Hz, it can be seen in the table 2 that the Peltier temperature stabilizer heats up or cools down the detector to almost the same extent as the object which is observed by the camera. This means that the Peltier stabilizer may deteriorate the performance of the thermal image and consequently, the technical requirements for a Pelter device must be very high. In the case of highly sensitive thermal imaging cameras, the temperature variation caused by the Peltier stabilizer must be at the level of 1 mK. In addition, the PWM control system should work at frequency of at least a few kHz to minimize the influence of the Peltier system on a microbolometer detector. It is worth noting that this problem increases as the distance between the sensor and the temperature stabilizer decreases.

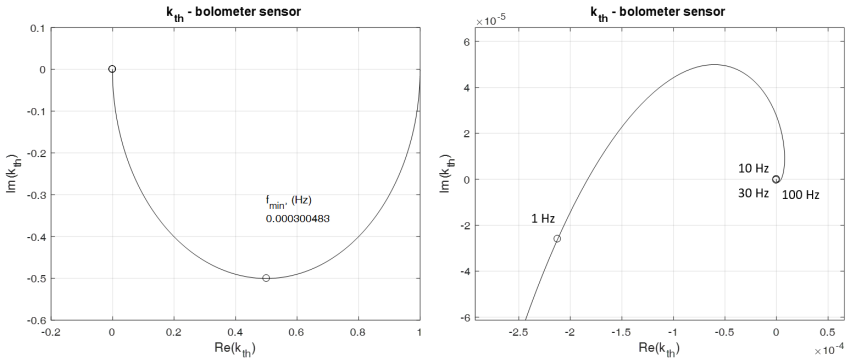

Fig. 4. *Thermal gain for the bolometer 640x480 matrix and cooled or heated by convection heat transfer through bottom surface of the heat sink*

Moreover, the heaters that are used more often today have a similar effect on the bolometer detector.

4. Conclusions

The article presents the theoretical analysis of the influence of the Peltier cell used to stabilize the temperature at the end of the heat sink thermally connected to the bolometric detector. To perform this analysis, the 1D thermal model was developed. The main conclusion of the analysis is that the quality of the temperature stabilization must be good enough not to degrade the performance of the bolometer detector. The presented analysis can be applied for thermal an mechanical optimisation the IR camera housing. The next stage of this research will be the experimental verification of the simulation results.

References

[1] Y.S. Kim, T.H. Kim, G.T. Kim, B.T. Lim, S.K. Lim, H.D. Lee, and G.W. Lee. Uncooled microbolometer arrays with high responsivity using meshed leg structure. *IEEE Photonics Technology Letters*, 25(21):2108–2110, 2013.

[2] U. Mizrahi, F. Schapiro, L. Bykov, A. Giladi, N. Shiloah, I. Pivnik, S. Elkind, S. Maayani, E. Mordechai, O. Farbman, Y. Hirsh, A. Twitto, M. Ben-Ezra, and A. Fraenkel. Advanced μ-bolometer detectors for high-end applications. *Proc. SPIE 8353, Infrared Technology and Applications XXXVIII, 83531H*, 2012.

[3] A. Rogalski. Infrared detectors. *CRC Press*, Second Edition:ISBN–10:142007671X, 2010.

[4] A. Fraenkel, U. Mizrahi, L. Bykov, A. Adin, Malkinson E., Zabar Y., Seter D., Gebil Y., and Kopolovich Z. Advanced features of scd's uncooled detectors. *Opto-Electronics Review*, 14:46–53, 01 2006.

[5] J.L.Tissot, C.Trouilleau, B.Fieque, A.Crastes, and O.Legras. Uncooled microbolometer detector: recent developments at ulis. *Opto-electronics Review*, 14(1):25–32, 2006.

[6] M. Strakowska, G. De Mey, B. Wiecek, and M. Strzelecki. A three layer model for the thermal impedance of the human skin: modelling and experimental measurements. *Journal of Mechanics in Medicine and Biology*, 15(4), 2015.

[7] M. Strakowska, P. Chatzipanagiotou, G. De Mey, V. Chatziathanasiou, and B. Wiecek. Multilayer thermal object identification in frequency domain using ir thermography and vector fitting. *International Journal of Circuit Theory and Applications*, 48(9):1523–1533, 2020.